The analysis of slightly distorted SAXS layer line patterns from fibrillar two-phase systems with short-range order*)

N. Stribeck

Institut für Technische und Makromolekulare Chemie der Universität Hamburg, Hamburg, FRG

Abstract: The information content of small-angle x-ray scattering from fibrillar two-phase systems under strain is discussed. The experimental background is a study of SBS star block copolymer samples during elongation using synchrotron radiation and a two-dimensional detector. The samples exhibit a layer line pattern with the slight indication of a four-point diagram. The theoretical considerations are verified using the experimental data.

Special scattering curves (sections and projections) can be extracted from the scattering pattern and are used to describe mathematical peculiarities of the pattern and their physical background. The scope of the paper covers product separability in cylindrical coordinates and an analysis of the separated factors. From the physical point of view information is gained on the validity of the approximation by a "one-dimensional fibrillar system" and the order within bundles of fibrils. An expression is given for the background scattering caused by an ensemble of non-identical oblong particles, organized in bundles of oriented fibrils. The difference in the information on the structure, obtainable from either section or projection, is discussed.

Key words: SAXS; layer-line pattern; drawing; block copolymers; synchrotron radiation

1. Introduction

In recent years, some work has been carried out in our institute to study thermoplastic rubber samples produced in a technical process far from thermodynamical equilibrium. Among other methods, we use synchrotron radiation to record two-dimensional SAXS patterns during the first draw cycle with a VIDICON detector at the Polymer Beamline, HASYLAB, Hamburg.

In the past, we studied samples of a linear SBS block copolymer, on which Polizzi and Bösecke [1] had observed the development of a layer-line pattern within an ellipsoidal envelope. Taking into account the observed phenomena as well as the former accuracy of the data, the author developed an adapted theoretical approach [2] for the evaluation of this scattering pattern. On the basis of this approach the data were analyzed (Stribeck et al. [3]).

Now, our interest has turned to SBS star block copolymers and this paper shall point out corresponding theoretical considerations. Figure 1 shows the typical SAXS intensity pattern of a SBS star block copolymer at a medium elongation. This three-dimensional (3D)-plot shall serve as a help to demonstrate the necessity of an advanced theoretical paper.

First, data accuracy of the patterns could be increased considerably since the older experiments. Thus, there is no longer the need to speculate on the power of Porods' law. We now can determine it after subtracting the fluctuation background, and are able to study the outer region of the SAXS pattern.

Second, the evaluation program has been ex-

*) Dedicated to Prof. Dr. Wilhelm Ruland on the occasion of his 65th birthday

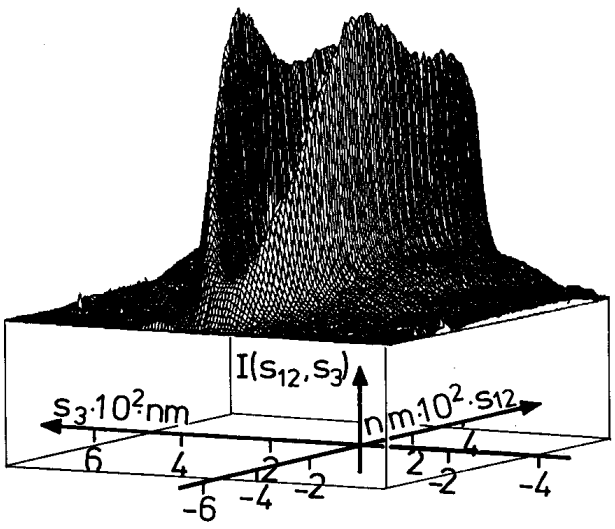

Fig. 1. SAXS intensity pattern of an SBS star block copolymer at an elongation $\varepsilon = 1.43$. Strain is parallel to s_3-direction. s_{12}, by convention, is a deliberate distance from the s_3-axis (cylindrical symmetry). The pattern was recorded using the SIT-VIDICON detector at HASYLAB, Hamburg. It shows the central part of the detector area of 512×512 pixels. A bordering region of 32 pixels width is omitted in the plot

tended. Thus, we now compute the projection of the intensity onto a line parallel to the direction of elongation, and we no longer need to postulate an ideal layer line pattern. Both sections and projections are accessible for analysis using our one-dimensional model function [2, 3].

Third, at medium elongation we, for the first time, observe some indication of a "four-point diagram". The layer lines show a dent in the central part, while they are somewhat bent at their ends. In the study of SBS block copolymers four-point-diagrams have been observed by several authors (Pakula et al. [4]; Séguéla and Prud'homme [5]).

2. Theoretical

2.1. General definitions

Let $\vec{r}$ be the position vector in physical space and $\vec{s}$ the scattering vector in reciprocal space with $|\vec{s}| = 2(\sin\theta/\lambda)$. λ is the wavelength of radiation, 2θ the scattering angle. Let $\Delta\rho_{el}(\vec{r})$, the electron density difference, be defined by $\Delta\rho_{el}(\vec{r}) = \rho_{el}(\vec{r}) - \langle\rho_{el}(\vec{r})\rangle_V$. $\langle\ \rangle_V$ denotes the average over the irradiated volume. Then the scattering intensity $I(\vec{s})$, arising from $\Delta\rho_{el}(\vec{r})$, is given by

$$I(\vec{s}) = \mathcal{F}(\Delta\rho_{el}^{*2}(\vec{r})) \tag{1}$$

with the 3D Fourier transform $\mathcal{F}(\ )$ being defined as

$$\mathcal{F}(g(\vec{r}))(\vec{s}) = \iiint g(\vec{r}) \cdot e^{2\pi i \vec{r}\vec{s}}\, d^3r\ . \tag{2}$$

The operator $*^2$ denotes the autocorrelation, and defining the 3D correlation function $\gamma(\vec{r})$, Eq. (1) can be written in the well known formulation

$$I(\vec{s}) = k \cdot \mathcal{F}(\gamma(\vec{r}))\ , \tag{3}$$

where the scattering power k is given by the integral of $I(\vec{s})$ over the whole reciprocal space. Thus, k reflects "the projection of the scattering intensity onto a point".

Let $I(\vec{s})$ show cylindrical symmetry

$$I(\vec{s}) = I(s_{12}, s_3)\ , \tag{4}$$

with s_{12} defining the radial and s_3 the axial component of the scattering vector. Under this assumption a convenient scattering curve I_{sc} is a section parallel to one of the coordinate axes

$$I_{sc}(s_3) = I(s_{12}, s_3)|_{s_{12}=\text{const.}}$$

or

$$I_{sc}(s_{12}) = I(s_{12}, s_3)|_{s_3=\text{const.}}\ . \tag{5}$$

Such a section can easily be extracted from the scattering pattern. The special sections through the origin of reciprocal space ("origin sections") shall be written as

$$\begin{aligned} \lceil I(\vec{s})\rceil_{s_{12}} &:= I(s_{12}, s_3)|_{s_{12}=0} = I(0, s_3) \\ \lceil I(\vec{s})\rceil_{s_3} &:= I(s_{12}, s_3)|_{s_3=0} = I(s_{12}, 0)\ . \end{aligned} \tag{6}$$

Other kinds of useful scattering curves can be generated from the scattering pattern by computing special projections. Let us define the projection of the scattering intensity $I(\vec{s})$ onto the s_3-axis by

$$\begin{aligned} \{I\}_{s_{12}}(s_3) &:= \int_{-\infty}^{\infty}\!\!\int I(\vec{s})\, ds_1\, ds_2 \\ &= 2\pi \cdot \int_0^{\infty} s_{12} \cdot I(s_{12}, s_3)\, ds_{12}\ . \end{aligned} \tag{7}$$

2.2. The SAXS layer-line pattern: Sections, projections, and product separability in cylindrical coordinates for a two-phase system

Under Fourier transformation projection and section exchange

$$\{I\}_{s_{12}}(s_3) = k \cdot \mathcal{F}_1(\lceil\gamma(\vec{r})\rceil_{r_{12}}(r_3))\ . \tag{8}$$

Here the operator $\mathcal{F}_1(\ )$ denotes the one-dimensional (1D) Fourier transformation. This theorem can help to interpret the projection of the intensity onto a line. Hence, the scattering curve $\{I\}_{s_{12}}(s_3)$ corresponds to the 1D correlation function $\lceil\gamma\rceil_{r_{12}}(r_3)$, which only collects all the correlations in r_3-direction of the structure in physical space.

Let us now assume this structure to be a two-phase system. Then, Eq. (8) yields that the intensity projection has to follow a 1D Porod law:

$$\lim_{s_3\to\infty}\{I\}_{s_{12}}(s_3) \propto s_3^{-2} . \tag{9}$$

Resuming these considerations, the intensity projection $\{I\}_{s_{12}}(s_3)$ is the correct scattering curve to extract structural information involving all the correlations along the principal axis of the fibrillar system.

As has been stated in previous studies [2, 3], it may be sufficient to analyze a deliberate section $I|_{s'_{12}}(s_3)$, if we can assume the intensity $I(\vec{s})$ to be product-separable in cylindrical coordinates

$$I(s_{12}, s_3) = f(s_{12})\cdot g(s_3) . \tag{10}$$

In this case the proportionality

$$\lceil I\rceil_{s_{12}} \propto I(\vec{s})|_{s'_{12}} \propto \{I\}_{s_{12}} \quad \forall\, s'_{12} \tag{11}$$

trivially holds. This product separability is a necessary condition for an ideal layer line pattern.

Equation (11) can be used to test the approximation of product separability by comparing section and projection. In doing this, we can even compare the Porod law of the section with that of the projection. An earlier paper [2] states that the intensity section $I(\vec{s})|_{s'_{12}}(s_3)$, too is expected to show a 1D Porod law within the observable region of reciprocal space. This should be true even in the case of imperfect orientation of the fibrils, if only the particles within the fibrils are not too anisotropic and, furthermore, these particles only show a short-range order along the fibrillar axis.

If this expectation can be verified, one should at least find a limited product separability in the "Porod law region", which means

$$I(\vec{s})|_{s'_{12}}(s_3) \propto \{I\}_{s_{12}}(s_3) \quad \text{for } |s_3| > s_{3p} , \tag{12}$$

or, with Eq. (9)

$$I(s_{12}, s_3) = A_p(s_{12})\cdot s_3^{-2} \quad \text{for } |s_3| > s_{3p} . \tag{13}$$

Here $A_p(s_{12})$, the "Porod asymptote", is denoted as in [2, 3]. s_{3p} shall be defined as the lower limit of the Porod region.

2.3. The shape of the factor $A_p(s_{12})$ and interfibrillar interaction

In a preceding paper ([3], Eq. (5)) the factor $A_{pd}(s_{12})$ was written as

$$A_{pd}(s_{12}) = n\cdot\frac{\Delta\rho_{el}^2\cdot S_{cl}^2}{2\pi^2}\cdot \mathrm{Jinc}^2(\pi d s_{12}) . \tag{14}$$

Here n is the number of particles in the sample, $\Delta\rho_{el}$ is the contrast of the two-phase system between particles and matrix, S_{cl} is the surface of the cylindrical particles lid, and d is their diameter. $\mathrm{Jinc}(x) := 2\cdot J_1(x)/x$ is a shortcut notation, where $J_1(x)$ is the first order Bessel function of first kind. A_{pd} stands for the "A_p-function of a dilute system".

$A_{pd}(s_{12})$ is proportional to the origin section in s_{12}-direction of the form factor scattering of n cylindrical domains. Equation (14) is valid for an ensemble of identical cylindrical particles which are perfectly orientated with their axes parallel to the r_3-direction. Moreover, no correlation among the particles is assumed in the r_{12}-plane. This assumption implies a very dilute system and thus in general only allows to describe the trend of $A_p(s_{12})$ in a rough approximation.

So let us refine this approximation, in order to obtain an expression which is adapted to an increased quality of experimental data. Therewith, we should keep in mind the constraints of the experimental determination of $A_p(s_{12})$. In the probable case that product separability is limited, the shape of the Porod asymptote must be extracted from an outer region of the scattering pattern, where intensity is low and, thus, the signal-to-noise ratio is poor. So we will not be able to record a detailed $A_p(s_{12})$-curve.

At least, one should give up the assumption of a dilute system, and thus deal with a "bundling of fibrils", i.e., the occupation of area by individual fibrils in the diametrical r_{12}-plane. To consider this effect, Porod [6] has derived a correction factor applicable to the above Eq. (14), which can describe the possible trend of $A_p(s_{12})$ for a concentrated system with sufficient accuracy

$$A_p(s_{12}) = A_{pd}(s_{12})\cdot C(s_{12}) , \tag{14b}$$

and

$$C(s_{12}) = \frac{1-\varepsilon_c^2}{1-2\varepsilon_c\cdot\cos(2\pi d s_{12})+\varepsilon_c^2} . \tag{15}$$

Here, ε_c is a parameter describing the "probability of contact" between neighboring fibrils. For $\varepsilon_c = 0$ there is neither attraction nor repulsion between

the fibrils and, additionally, the shape of the fibrils lids allows a tiling of the r_{12}-plane (i.e., a filling without intermediate area). In this case, we find the undisturbed law for $A_p(s_{12})$, even for a concentrated system. According to Porod, $\varepsilon_c < 0$ means a tendency to separate, and then $A_p(s_{12})$ will be varied towards "liquid scattering". If a tiling of the r_{12}-plane is possible and the fibrils show a tendency to aggregate, ε_c will be positive and $A_p(s_{12})$ will be altered towards the typical "gas scattering".

Figure 2 shows the variation of this model function $A_p(s_{12})$ for several chosen values of ε_c. We observe that only in the case of gas scattering is the outer part of the curve lowered, while in the case of a segregation tendency the intensity in the central part is decreased at the expense of a growing peak.

Neither by using ideal nor by using distorted cylindrical domains (for a visualization cf. Spontak et al. [7]) it should be possible to tile the r_{12}-plane. Thus, liquid scattering is most probable to occur. In a real system, we will not only observe distortions of particle shape (here: fibril shape), but also a distribution of sizes (here: fibril diameters). As has been shown in an earlier paper [2], the function $\mathrm{Jinc}(x)$ can be approximated by the function $\mathrm{sinc}(x) := \sin(x)/x$ in the observable region of the scattering pattern, if we take into account a minor rescaling with a factor 1.17. If we furthermore assume the diameter distribution of the particles to

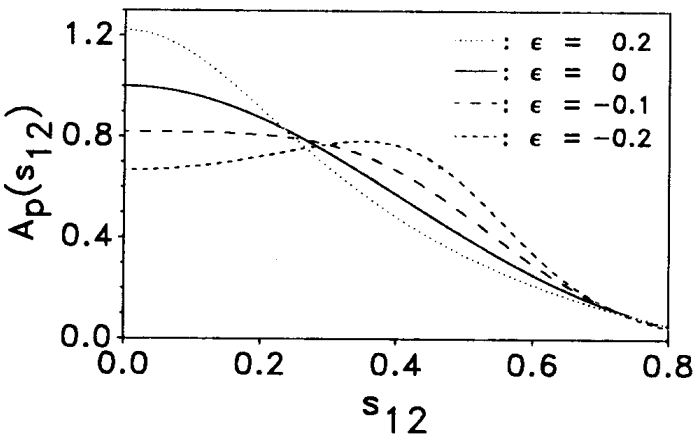

Fig. 2. Shape variation of the model form factor scattering $A_p(s_{12})$ according to Eqs. (14b) and (15) with Porod's ε_c-parameter concerning the "probability of contact". Positive ε_c means agglomeration (gas scattering), negative ε_c separation of fibrils (liquid scattering). For $\varepsilon_c = -0.1$, we find a nearly trapezoidal shape of $A_p(s_{12})$. The solid line shows the unaffected form factor scattering ($\varepsilon_c = 0$)

be a Gaussian function, we can proceed like in [2] and write for $A_{pd}(s_{12})$

$$A_{pd}(s_{12}) = n \cdot \left[\frac{\Delta\rho_{el} \cdot d \cdot 1.17}{8\pi}\right]^2 \cdot \frac{1}{s_{12}^2} \cdot (1 - \cos(2\pi d^* s_{12}) \cdot \exp(-2\pi^2 \sigma_d^2 s_{12}^2)) \,. \quad (16)$$

$d^* := d/1.17$, with d being the mean fibrillar diameter. σ_d is the variance of the Gaussian distribution of the fibril diameters.

One finds that the tail of $A_p(s_{12})$ may be severely damped in the case of a broad distribution of diameters. This damping would be enhanced if gas scattering would occur and would be partly compensated in the case of a decreased probability of contact among the fibrils (liquid scattering).

In the preceding discussion we have neglected any effects of fibrillar arrangement with respect to the r_{12}-plane. If we had such an order of placing, we should evaluate the function $A_p(s_{12})$ in the standard way, i.e., determining a "long period". Moreover, if it were possible to obtain precise data, one could even compute and analyze the correlation function in the r_{12}-plane (cf. Vonk [8]).

Under certain circumstances it is possible to decide whether or not the bundled fibrils are arranged. Let us consider a rubbery system, where we can assume the volume of the sample to be constant during elongation. Let us furthermore assume that after initial drawing fibrils have been formed and that we observe at least limited product separability of the scattering pattern, as has been discussed before.

Then, if $A_p(s_{12})$ is governed by the arrangement of the fibrils, we should observe a variation of this function with increasing strain. A transversal "long period" L_t should decrease according to $L_t = \lambda^{-1/2} \cdot L_0$, where L_0 is some initial long period and λ is the draw ratio. If we cannot observe a variation of $A_p(s_{12})$ with λ, the fibrils in the bundle can be considered to be placed irregularly.

2.4. Particle form factor and interpretation of a "4-point-pattern"

In the last section we discussed the transversal factor $A_p(s_{12})$, a function which is likely to be dominated by the form factor scattering and some influence of fibril bundling. For a two-phase system with only short range order the interparticular

interferences along the fibrillar axis should fade away within a limited interval around the primary beam. Demanding product separability we thus find an approximation for a scattering background $B_p(s_{12}, s_3)$ in both radial and axial directions, taking into account bundling of fibrils as well as the mean form factor scattering of an ensemble of orientated cylinders in which dimensions of the individual particles vary according to Gaussian statistics

$$B_p(s_{12}, s_3) = F(s_{12}, s_3) \cdot C(s_{12}) \,, \tag{17}$$

with

$$\begin{aligned} F(s_{12}, s_3) = n \cdot \left[\frac{\Delta\rho_{el} \cdot d \cdot 1.17}{8\pi}\right]^2 \cdot \\ \cdot [s_{12}^{-2} \cdot (1 - \cos(2\pi d^* s_{12}) \\ \cdot \exp(-2\pi^2 \sigma_d^2 s_{12}^2))] \\ \cdot [s_3^{-2} \cdot (1 - \cos(2\pi h s_3) \\ \cdot \exp(-2\pi^2 \sigma_h^2 s_3^2))] \,. \end{aligned} \tag{18}$$

h is the mean cylinder height and σ_h the variance of the Gaussian distribution of the heights ($d^* = d/1.17$, cf. Eq. (16)).

Thus, we should keep in mind that evaluating the ellipsoidal envelope of the scattering pattern to get information on the anisotropy of the cylindrical particles, as has been proposed in [2], only then is a fair approximation if the variation of cylinder heights is comparable in amount to that of the cylinder diameters. Moreover, both the dimension distributions should be unimodal.

During the straining of thermoplastic rubber material some authors have observed a four-point diagram (Pakula et al. [4], Séguéla and Prud'homme [5]), and convincingly interpreted their data as the result of a superposition of form factor and lattice factor. An example of such a structure is shown in Fig. 3a. Due to a constant tilt of the cylinders with respect to the fibrillar axis, the two narrow and tilted beams of the form factor cut four points out of the lattice factors layer lines. Since form-factor scattering always dominates at larger $|\vec{s}|$ for a system with a limited range of order, such a structure must have a scattering pattern where the intensity concentrates within four leaves.

Another possibility to break up the layer lines into two points each is shown in Fig. 3b. Here the four-point diagram is just an effect of the "lattice factor", due to some kind of "monoclinic macrolattice" (cf. Fronk and Wilke [9]). In this case, we should not observe four leaflets of intensity, but a convex form factor envelope containing layer lines with a dent in the middle.

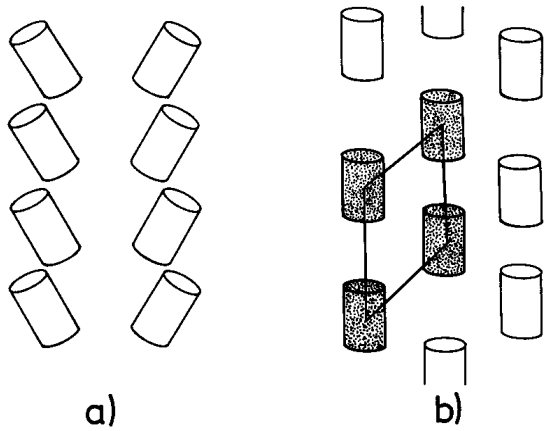

Fig. 3. Model structures resulting in a SAXS 4-point pattern. a) Pattern created by a superposition of form factor (tilt cylinders) and one-dimensional lattice (fibril). b) Pattern created by a three-dimensional lattice factor ("monoclinic macrolattice", correlated fibrils)

3. Experimental verification and discussion

3.1. The general type of the "four-point-diagram"

Figure 1 shows one of the most pronounced "four-point-diagrams" from the series of SBS star block copolymers. According to the preceding discussion it appears reasonable to assume that correlation of adjacent fibrils causes the layer-lines dent as well as its bending in the outer region. A diagram with four peaks which are more or less separated was never observed.

The assumed transversal correlation of fibrils can be explained from the four-star topology of the macromolecules. Some of the macromolecules should at least connect three different poly(styrene) domains, so that under strain adjacent fibrils should partly be arranged in the way outlined in Fig. 3b.

3.2. Comparison of projection and section

Figure 4 shows an experimental projection $\{I\}_{s_{12}}(s_3)$ (solid line) and the corresponding section

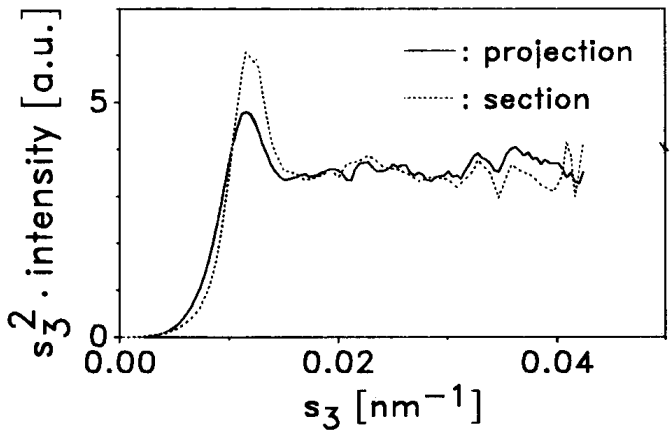

Fig. 4. Experimental SAXS intensity projection and section in a plot revealing a one-dimensional Porod law. The sample is a SBS star block copolymer at an elongation $\varepsilon = 1.43$. The same constant density fluctuation background was subtracted from both curves before multiplication with s_3^2

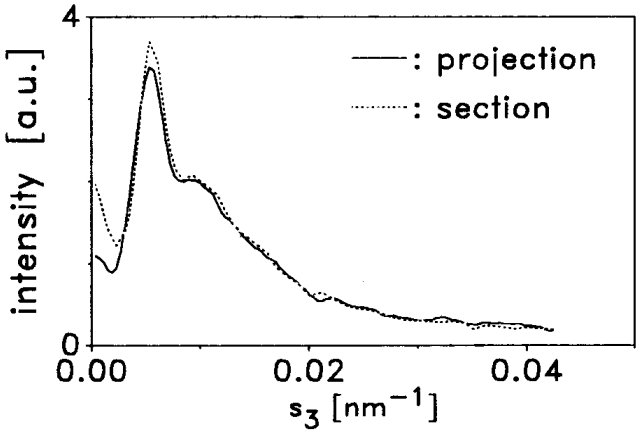

Fig. 5. Experimental SAXS intensity projection and section. The sample is an SBS star block copolymer at an elongation $\varepsilon = 5.81$

$I|_{s'_{12}}(s_3)$, $s'_{12} = 0.019$/nm (dotted line), multiplied by s_3^2 after subtracting a constant density fluctuation background. Both curves are extracted from the scattering pattern shown in Fig. 1.

We notice the distinct difference between projection and section in the region of the long-period reflection, while the tail of the curves follows a long and perfect 1D Porod law. Within the Porod region both curves are identical, and this is the proof for the discussed limited product separability. The section in the plot has been multiplied by a chosen factor, so that the curves match in the Porod region. Taking into account for this factor, even the subtracted fluctuation background constant is the same for projection and section.

Only the assumption of a one-dimensional Porod law linearizes the tail of both the scattering curves. Thus, we conclude that we are allowed to treat our scattering patterns in terms of a system of perfectly orientated fibrils.

All the scattering patterns of the studied samples show these characteristics, if only the relation $\varepsilon \geq 1$ is fulfilled for the elongation ($\varepsilon := \lambda - 1$, λ is the draw ratio). With increasing strain the difference between projection and section at the beginning of the curves decreases (see Fig. 5), but it never vanishes. Hence, for the study of the present star block copolymers, the assumption of an ideal layer line pattern (i.e. full product separability) is insufficient. This means, that one should analyze the projection $\{I\}_{s_{12}}(s_3)$, if one intends to study "the average fibrils one-dimensional structure".

On the other hand, section $I|_{s'_{12}}(s_3)$ should contain some kind of a weighted average over the 1D structure, where the weighting distribution is a function of the cutting position s'_{12}. We can confine this diffuse statement, if we make an assumption on the structure evoking the scattering pattern. Let us assume that part of the fibrils appear uncorrelated in radial direction, while in another part of the irradiated volume fibrils are correlated and appear to form a "monoclinic macrolattice" according to Fig. 3b. If we then cut through the maximum intensity of the layer line, we increase the weight of the macrolattice component at the cost of the component containing the uncorrelated fibrils.

3.3. *Analysis of $A_p(s_{12})$ and the arrangement of the fibril rods in the r_{12}-plane*

Figures 6 and 7 show experimental curves $A_p(s_{12})$ of the same SBS star block copolymer at different elongations (Fig. 6: $\varepsilon = 1.43$; Fig. 7: $\varepsilon = 3.38$). Each of the drawings contains four different curves. These curves are sections $s_3'^2 \cdot I(\vec{s})|_{s'_3}(s_{12})$ of the scattering pattern, taken from the Porod region in s_{12}-direction at different positions s'_3. Dark symbols denote a section in the beginning of the Porod region (i.e., small s'_3), light symbols denote a section towards the end of the region where the one-dimensional Porod law is valid. The fact that multiplication by the constant

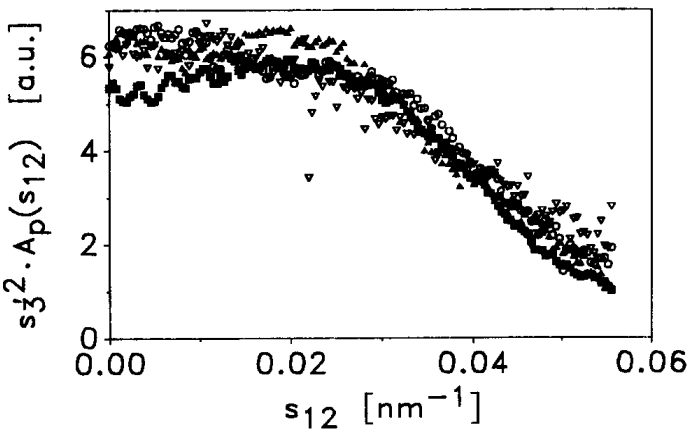

Fig. 6. SBS star block copolymer at an elongation of $\varepsilon = 1.43$: Experimental $A_p(s_{12})$-curves from the "Porod region in s_3-direction" at different positions s_3'. (■): $s_3' = 0.018$/nm. (▲): $s_3' = 0.022$/nm. (○): $s_3' = 0.026$/nm. (▽): $s_3' = 0.030$/nm

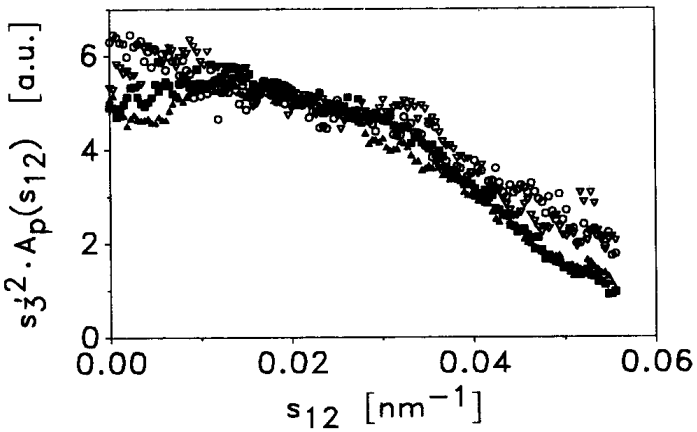

Fig. 7. SBS star block copolymer at an elongation of $\varepsilon = 3.38$: Experimental $A_p(s_{12})$-curves from the "Porod region in s_3-direction" at different positions s_3'. (■): $s_3' = 0.016$/nm. (▲): $s_3' = 0.020$/nm. (○): $s_3' = 0.024$/nm. (▽): $s_3' = 0.028$/nm

$s_3'^2$ scales all the curves onto one master curve again reflects the validity of the 1D Porod law.

Because of the fact that the data are taken from the outer region of the scattering pattern, the signal-to-noise ratio is only fair and even decreases with increasing s_3' and increasing elongation ε.

We compare the shape of the experimental curves with the model curves plotted in Fig. 2 and find that the experimental data are similar to the "trapezoidal" model curve with a contact parameter $\varepsilon_c = -0.1$. The observed curves show a distinct bending point, but no maximum.

If we simply approximate the measured curves by a trapezoid, its only parameters are the position of the bending point s_{12_b} and the half length s_{12_l} of the trapezoids basis. An evaluation of these parameters yields a bending point position of $s_{12_b} \approx 0.028$/nm and $s_{12_l} \approx 0.06$/nm, independent from strain.

According to the considerations in the theoretical part of this paper, we thus regard the fibrils in the bundle to be placed irregularly within the r_{12}-plane, since in this case the shape of $A_p(s_{12})$ is no function of the population density.

4. Conclusions

The theoretical considerations of this paper concern the information content of the scattering from fibrillar two-phase systems under strain. If one observes at least a limited product separability of the small-angle scattering pattern, the observable Porod law has to be one-dimensional. In this case the structural model of perfectly orientated bundles of fibrils appears to be a good approximation for the description of the SAXS.

A non-ideal layer-line pattern in this case is most probably caused by interparticular interferences among the fibrils in the bundle, as well as by a dispersion of the fibril structures, if one compares different bundles. Thus, the different information content of sections and projection should mainly be an effect of weighting these structures. While the projection does have the uniform weighting of the 1D structure, a section may favor a fraction of well-ordered fibrillar bundles.

If the fibrils show a short-range order only, and the fibrils are bundled without any preference of distance or order, the outer part of the scattering pattern is dominated by a background scattering. This background describes the particle dimensions, their dispersion and, according to Porod [6], the tendency of neighboring fibrils to aggregate or to separate. For the special case of unimodal Gaussian dimension statistics of oblong particles, this background can be presented as an analytical expression.

An application of these theoretical results to a series of SAXS patterns obtained from SBS star block copolymers is possible. For these samples a quantitative analysis of the structure as a function

of strain will be published in a following paper [10].

Acknowledgements

The author is indebted to Dipl. Eng. Paul Ghioca and Dr. Emil Buzdugan from the Chemical Research Institute ICECHIM, Bucharest, Romania, for sample preparation and valuable discussions. Many thanks to Dr. Rüdiger Zietz, for the excellent supervision at the "Polymer Beamline" of HASYLAB, concerning the whole experiment, data preprocessing and, especially, the drawing machine. Many thanks as well to Dipl. Phys. Clemens Schulze for supervision of the SIT-Vidicon-detector, and to Ding Yi Hong for cooperation during experiment.

Development of the SIT-Vidicon-system was funded by BMFT, the German Federal Ministry for Research and Technology under contract number 05305HXB.

References

1. Polizzi S, Bösecke P, Stribeck N, Zachmann HG, Zietz R, Bordeianu R (1990) Polymer 31:638–645
2. Stribeck N (1989) Colloid Polym Sci 267:301–310
3. Stribeck N, Bösecke P, Polizzi S (1989) Colloid Polym Sci 267:687–701
4. Pakula T, Saijo K, Kawai H, Hashimoto T (1985) Macromolecules 18:1294–1302
5. Séguéla R, Prud'homme J (1988) Macromolecules 21:635–643
6. Porod G (1972) Monatshefte für Chemie 103:395–405
7. Spontak RJ, Williams MC, Agard DA (1988) Polymer 29:387–395

8a. Vonk CG (1989) In Baltá Calleja FJ, Vonk CG (eds) X-ray scattering of synthetic polymers. Elsevier, Amsterdam, pp 298–303

8b. Vonk CG (1979) Colloid Polym Sci 257:1021–1032

9. Fronk W, Wilke W (1985) Colloid Polym Sci 263:97–108
10. Stribeck N, Hong DY, Zietz R, Zachmann HG, Petermann J, Ghioca P, Buzdugan E (1991) to be published

Received November 13, 1990;
accepted March 15, 1991

Author's address:

Dr. N. Stribeck
Institut TMC
Bundesstr. 45
2000 Hamburg 13, FRG